Influence of Taheri Consciousness Bond Field on the Crystallization and Strength of Cement Mortar (Concrete)

Bahareh Kazazi[1*], Mohammad Ali Taheri[2]

1. Civil Engineering, CEO of Hoobe Construction Company, Tehran, Iran.

2. Sciencefact R&D Department, Cosmointel Inc. Research Center, Ontario, Canada.

ABSTRACT

In this study, the behavior of cement mortar was investigated under the Consciousness Bond Field. Taheri Consciousness Fields (TCFs) were founded and introduced by Mohammad Ali Taheri as new Fields more than four decades ago. These Fields are neither material nor energetic. Therefore, they do not have quantity, but they have direct effects on both matter and energy. In other words, although TCFs cannot be directly measured, we can investigate their effects indirectly through various reproducible experiments. In all tests of this research, type II cement and standard sand were used. The samples preparation and their strength measurement were done under the ISIR 393 standard, and each group included 3 prism samples. Three series of experiments were performed with a number of different groups, in each series one group was as control and the others were the study samples under the effect of Consciousness Bond Field. Series 1 included five groups of cement sand mortar. Compres-sive and flexural strengths were measured at 7, 28, and 42 days of age. Series 2 included four groups of cement sand mortar which were measured at 7, 28, and 42 days of age. Series 3 included four groups of cement sand mortar made exactly according to the above-said condition. And strength was measured at 7, 28, 42, and 90 days of age. Due to the results received from FT-IR (Fourier-transform infrared spectros-copy), SEM (Scanning electron microscopy), XRF (X-Ray Fluorescence), and XRD (X-ray Diffraction), the growth trend of the strength of the samples under the Consciousness Bond Field were more significant than the control samples. The results of other analyzes showed that the abundance of chemical compounds containing calcium (CaCO3 from 20 to 80% and Ca3SiO5 from 25 to 75%) in the samples under the Consciousness Bond Field at 90 days was higher than the control. While silicon-containing compounds were higher in control samples at the same age. Sodium (Na), Potassium (K), and Phosphorus (P) were reduced by approximately (an average of 30%) in samples under Con-sciousness Bond Field at 90 days, while the abundance of Aluminum and Calcium was increased (about 7% on average). Differences in the appearance and chemical composition of the crystals, including the amount of ettringite formation in the samples under the Conscious-ness Bond Field, were observable in SEM imaging.

* Corresponding author:

Bahareh Kazazi
Civil Engineering, CEO of Hoobe Construction Company, Tehran, Iran.

Email: baharkazazi@gmail.com

Keywords: Cement-sand mortar, Consciousness Bond Field, Taheri Consciousness Fields, the strength of cement

INTRODUCTION

Cement was invented in 1824 and no material has been able to replace it yet [1]. The combination of aggregate cement and water as concrete is one of the most widely used materials in the world, and more than 4 million tons of cement is produced annually in the world [2]. Due to the dependence of industry on the properties of this material, various methods are offered to increase its efficiency. It should be noted that the first performance of this material is hardening which is out of chemical reactions. Because of the importance of cement, the study of its changes trend under the Consciousness Bond Field was the subject of this study. Consciousness Bond Field is expected to increase chemical reactions of the composites and improve their behavior in direction of their fundamental character (According to the Theory of General Connection of Particles introduced by Taheri) [3].

To get acquainted with the theoretical foundations of T-Consciousness Fields, it is worth mentioning that The nature of consciousness and its place in science has received much attention in the current century. Many philosophical and scientific theories have been proposed in this area. In the1980s, Mohammad Ali Taheri introduced novel fields with a non-material/non-energetic nature named Taheri Consciousness Fields (TCFs). In this perspective, T-Consciousness is one of the three existing elements of the universe apart from matter and energy. According to this theory, there are various TCFs with different functions, which are the subcategories of a networked universal internet called the Cosmic Consciousness Network (CCN). The major difference between the theory of TCFs and other theoretical concepts about consciousness is related to the practical application of the TCFs. TCFs can be applied to all living and non-living creatures, including plants, animals, microorganisms, materials, etc.

Mohammad Ali Taheri, the founder of Erfan Keyhani Halqeh, a school of thought, introduced a new science in 2020 as a branch of this school. He coined the term Sciencefact for this new science because it utilizes scientific investigations to prove the existence of T-Consciousness as an irrefutable phenomenon and a fact. Although science focuses solely on the study of matter and energy and Sciencefact, by contrast, explores the effects of the [non-material/non-energetic] TCFs, Sciencefact has provided a common ground between the two by conducting reproducible laboratory experiments in various scientific fields, and it has used the scientific approach in proving TCFs.

The influence of the TCFs begins with the Connection between CCN as the Whole Taheri Consciousness of the universe and the subjects of study as a part. This Connection called “Ettesal” is established by a certified and trained individual who has been entrusted with the TCFs. The human mind has an intermediary role (Announcer) which plays a part by fleeting attention to the subject of study and then the main achievement obtained as a result of the effects of the TCFs. These Fields cannot be directly measured by science, but it is possible to investigate their effects on various subjects through reproducible laboratory experiments.

The research methodology in the study of T-Consciousness has been founded on the process of Assumption, Argument, and Proof, in which the basic Assumption is: The Cosmos was formed by a third element called T-Consciousness that is different from matter and energy.

The Argument: The existence of TCFs can be demonstrated by its effects on matter and energy (e.g., humans, animals, plants, microor-

ganisms, cells, materials, etc.)

The Proof: is the scientific verification of the effects of TCFs on matter and energy (according to the Argument) through various reproducible scientific experiments.

Accordingly, to investigate and verify the existence, effects, and mechanisms of TCFs, the following five research phases (Phases 0 through 4), and the aims of each phase are outlined below.

Phase-0 studies aim to prove the existence of TCFs by observing their effects. The nature of T-Consciousness and what it is will not be addressed in this phase. Phase-1 explores the varied effects of different TCFs. Phase-2 examines the reason behind the varied effects of these fields. Phase-3 investigates the mechanism of TCFs effects on matter and energy. Finally, Phase-4 draws significant conclusions, particularly with regard to the mind and memory of matter and their relation to the T-Consciousness, etc. [4-6]

Materials and methods

Preparation of cement mortar and evaluation of increase in their strength in all tests were based on ISIR 393 [7]. In all samples, standard sand and type II cement were used. And all of them made samples were kept in exactly the same environmental conditions from the beginning to the strength measurement.

According to the above standard, the method of measuring flexural and compressive strength was determined with prism samples with dimensions of 160 × 40 × 40 mm. These samples were molded using a paste mixture consisting of one weight unit of standard sand and one-half weight unit of water (water to cement ratio 0.05). To determine the flexural strength, a three-point loading device was used in which the prism sample was inserted into the machine from the side that was in contact with the mold, and then the load was applied to the opposite sides of the prism by a high roller at a speed of 50 ± 10 N /S until the sample was broken. The two prism samples were then covered with a damp cloth until the compressive strength test was performed.

Flexural strength R_f was calculated according to the following equation:

$$R_f = b^3 / L \times F_f \times 1.5$$

where R_f: Flexural strength in Mpa

b: Dimensions of the square section of the prism in millimeters

Ff: The load applied to the prism at the time of failure in N

L: The distance from the center to the center of the rollers or loading openings in millimeters.

For measuring the compressive strength, the test was performed on half of the flexural strength samples. Each sample was placed inside the machine and the load was gently applied to the sample at a speed of 2400 ± 20 N/S until the sample was broken.

Compressive strength in Mpa was calculated from the following equation:

where

$$R_C = F_C / 1600$$

R_C: Compressive strength in Mpa

F_c: Maximum load during failure in Newton and

1600: The surface of the loading jaw or the surface of the auxiliary plates (40 × 40 mm) in square millimeters.

The results of the flexural strength test were calculated according to the numerical mean of three unique results and each test was reported with an approximation of 0.1 Mpa and the numerical average of the results of the three tests was reported with an approximation of 0.1 Mpa.

group was calculated for the compressive strength. Each result was presented with an approximation of 0.1 Mpa and was obtained by performing six compressive strength tests on three broken prisms. If each of the six results alone was more than 10% different from the average, it was removed and the average of the remaining five samples was presented. And if one of the results of the five samples differed by more than 10% from the numerical average, all results were deleted, and no result was provided for that group [7].

Naming the samples

Before preparing the samples, each group of molds was named randomly and by meaning-less names by the laboratory manager. One group was considered as the control and the rest as experimental. The names were declared to the administrator of establishing TCF.

Application of Taheri Consciousness Fields

One of the introduced TCFs is called the Consciousness Bond Field and was applied to the samples according to the protocols regulated by the COSMOintel research center (www.COSMOintel.com). A request for Connection to the CCN to utilize TCFs can be placed through the COSMOintel website in the "Assign An-nouncement" section. This access is availa ble for everyone at no cost. In order to study and experience this Connection, the researchers can register on the website at any time in order to report the experiment to the COSMOintel research center. Certain details of the experiment must be provided to the center; for example, the characteristics or number and name of samples and controls must be specified. This entire experiment was carried out as a double-blind method where lab technicians were completely unaware of the TCFs.

Flexural and compressive strength measurement test - Series 1

Five groups of cement sand mortar were prepared according to the mentioned standard and conditions, each group consisted of three samples. They were all kept in exactly the same physical and environmental conditions such as temperature, humidity, and pressure. Then compressive and flexural strengths were measured at the ages of 7, 28, and 42 days.

Flexural and compressive strength measurement test - Series 2

Four groups of cement mortar were prepared according to the above-mentioned standard and conditions, each group containing three samples. The strength was measured at the ages of 7, 28, and 42 days.

Flexural and compressive strength measurement test – Series 3

Four groups of cement-sand mortar, each group consisting of three samples, were made exactly in accordance with the mentioned conditions. Their strengths were measured at the ages of 7, 28, 42 and 90 days. FT-IR (Fourier-transform infrared spectros-copy) was analyzed at the ages of 28, 42, and 90 days. And SEM (Scanning electron micros-c opy), XRF (X-Ray Fluorescence), and XRD (X-ray Diffraction), analyses were conducted at the age of 90 days.

Results and discussion

Strength measurement of all samples

Table 1 . The measured flexural and compressive strengths.

	Name	Flexural strength (Mpa) Age-day				Compressive strength (Mpa) Age-day			
		7	28	42	90	7	28	42	90
series 1	B-control	*	7.3	7.1		29.5	46.9	42.9	
	A	6.1	7.5	7.7		34.8	51.2	47.2	
	F	6.1	7	7.1		32	45.8	46.6	
	a	5.5	7.2	7.6		29.1	38.8	48.6	
	b	5.6	7	7.7		29.3	44.3	56	
Series 2	SH-control	6.1	9.05	10.8		31.7	45.6	48.8	
	A1	6	8.1	10.7		31	45.1	52	
	B1	6.1	*	10.8		30.2	44.5	51.5	
	C1	*	*	10.7		29.3	44.4	49.5	
series 3	Sh-control	7.5	8.1	8.2	8.6	32.5	41.4	42.8	45.9
	a1	7.3	8.6	8.3	8.8	31.4	42.1	41.8	48.1
	b1	7	8.2	8.3	8.7	30.8	41.7	44.3	47.8
	c1	7.5	8.1	7.7	7.9	31.8	44.7	44	46.4

Table 2 . Percentage of change in compressive and flexural strengths compared to the 7-day-old age of the samples in their own group.

	Name	Percentage change of flexural strength Age-day				Percentage change in compressive strength Age-day			
		7	28	42	90	7	28	42	90
series1	B-Control	*	7.30%	7.10%		*	59%	45.40%	
	A	*	23%	26.20%		*	47.10%	35.60%	
	F	*	14.75%	16.40%		*	43.10%	45.60%	
	a	*	31%	38.20%		*	33.33%	67%	
	b	*	26.80%	37.50%		*	51.20%	91.10%	
series 2	SH-Control	*	48.30%	77%		*	43.80%	53.90%	
	A1	*	35%	78%		*	45.50%	67.70%	
	B1	*	*	77%		*	47.40%	70.52%	
	C1	*	*	*		*	51.50%	69%	
series 3	Sh-Control	*	8%	9.30%	14.665	*	27.40%	31.70%	41.23%
	a1	*	17.80%	13.70%	20.50%	*	34.10%	33.12%	53.18%
	b1	*	17.14%	8.57%	24.30%	*	35.40%	43.80%	55.20%
	c1	*	8%	3%	5.30%	*	40.56%	38.36%	46%

Considering the way of presenting the results based on the used standard, some samples have been removed at the discretion of the test technician and taking the test error into account. As shown in the tables, in the samples of Series 1, the increase in strength started from the first measurement at the age of 7 days. While the samples of other Series showed a decrease in strength at the age of 7 days in subsequent measurements the growth rate of strength increased compared to the age of 7 days.

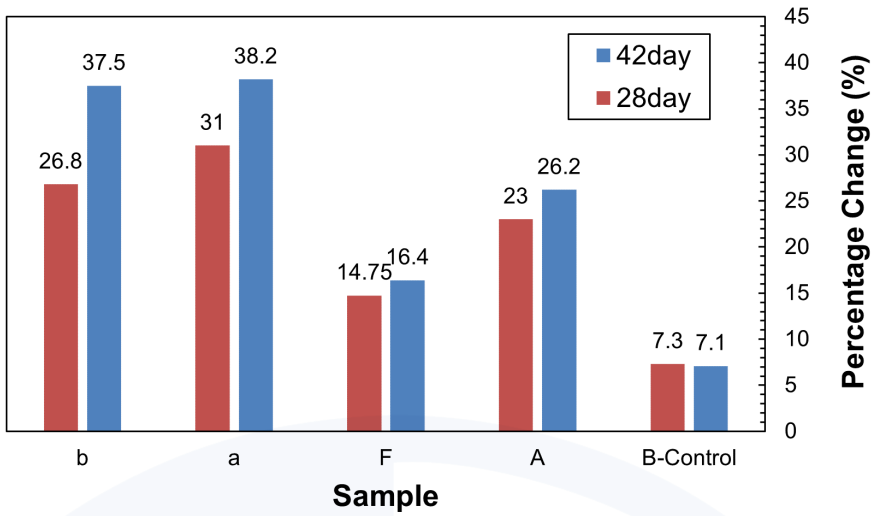

Figure 1- Percentage of flexural strength growth in Series 1 compared to seven-day age in its own group

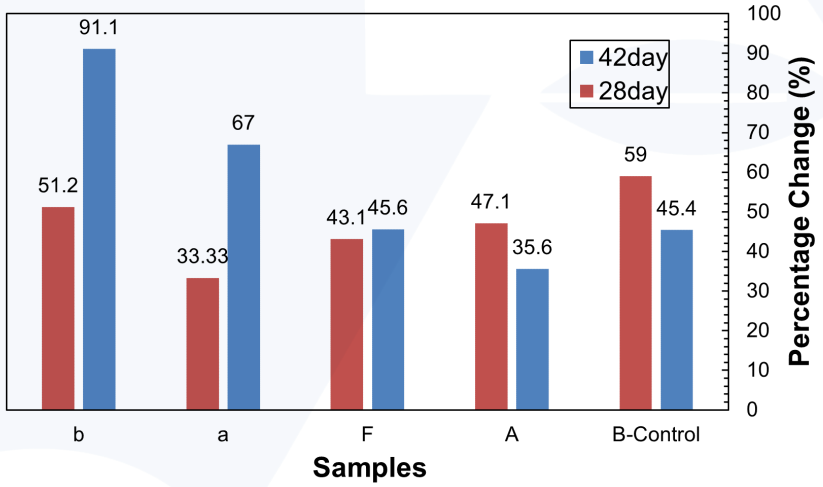

Figure 2- Percentage of compressive strength growth in Series 1 compared to seven-day age in its own group

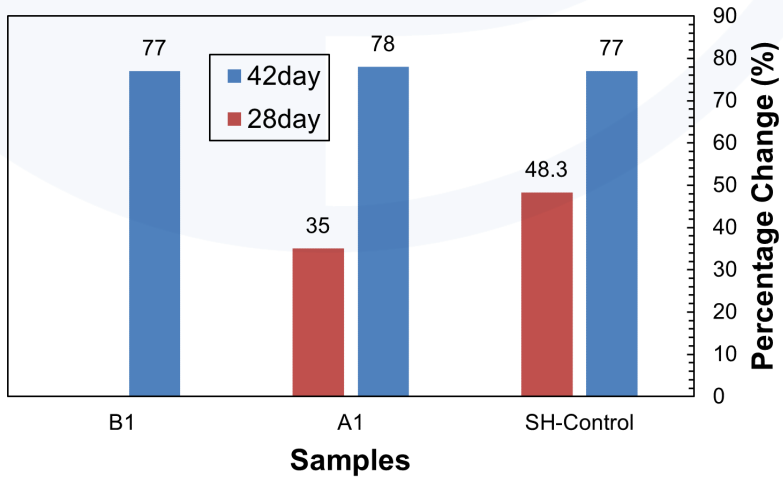

Figure 3- Percentage of flexural strength growth in Series 2 compared to seven-day age in its own group

Vol. 01
No. 07
April
2022

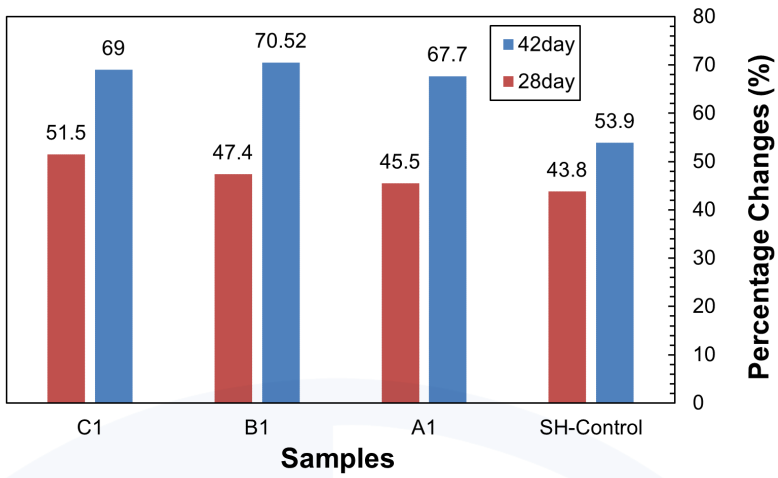

Figure 4- Percentage of compressive strength growth in Series 2 compared to seven-day age in its own group

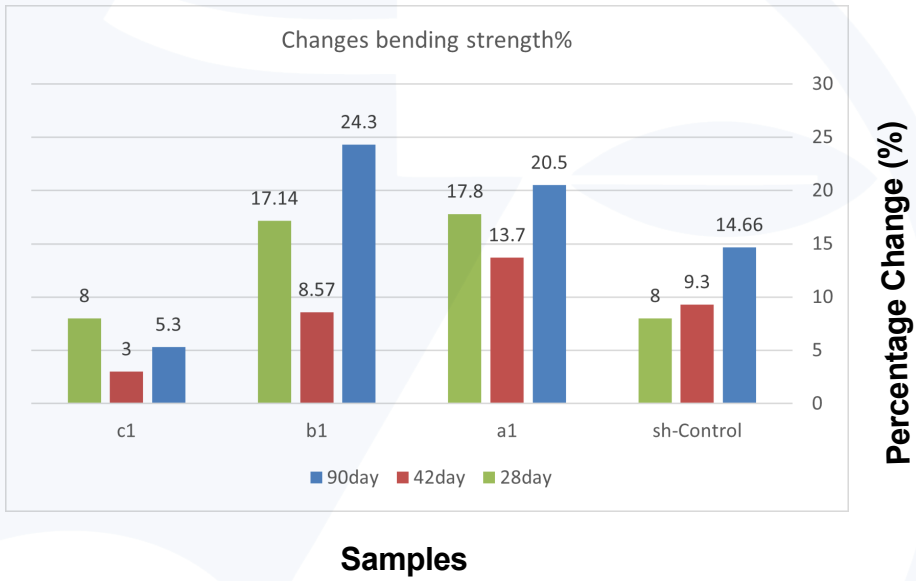

Figure 5- Percentage of flexural strength growth in Series 3 compared to seven-day age in its own group

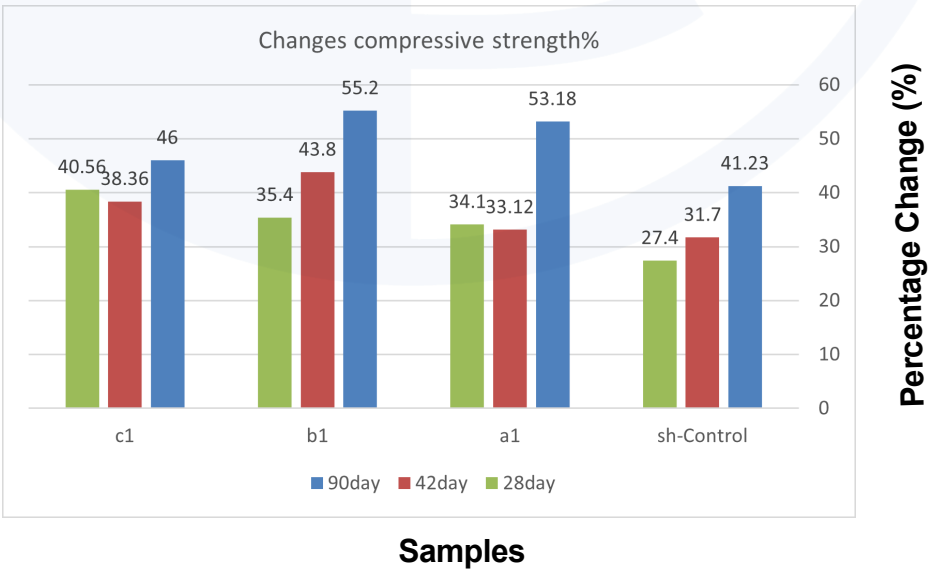

Figure 6- Percentage of compressive strength growth in Series 3 compared to the seven-day age in its own group

As seen, in most samples under TCF, the growth rate of strength over time compared to the age of 7 days was more than the control samples. This phenomenon indicates changes in the structure of chemical compounds. Also, in recent years, due to the environmental pollution caused by cement, the use of cement with new and green chemical compounds has flourished to replace Portland cement in the industry [8], which the growth pattern of their strength is different from the known Portland cement used in this study. For example, Lc3-50 cement, which is going to be replaced by Portland cement in the industry [8], shows a decrease in strength in the first days and then in the ages of 28 to 42 days shows more strong growth and again in 90 days shows a decrease in strength compared to Portland cement [8-9]. The TCF may have intelligent-ly altered the behavior of the cement.

FT-IR analysis of the samples - Series 3

To investigate the chemical structure of cement mortar, FT-IR test was used, and the results are shown in the figure 7. Also, to compare the results better, the magnified image of these spectra in the range of 400 cm^{-1} to 1800 cm-1 is shown.

In all graphs, the control samples are demarked as "Sh".

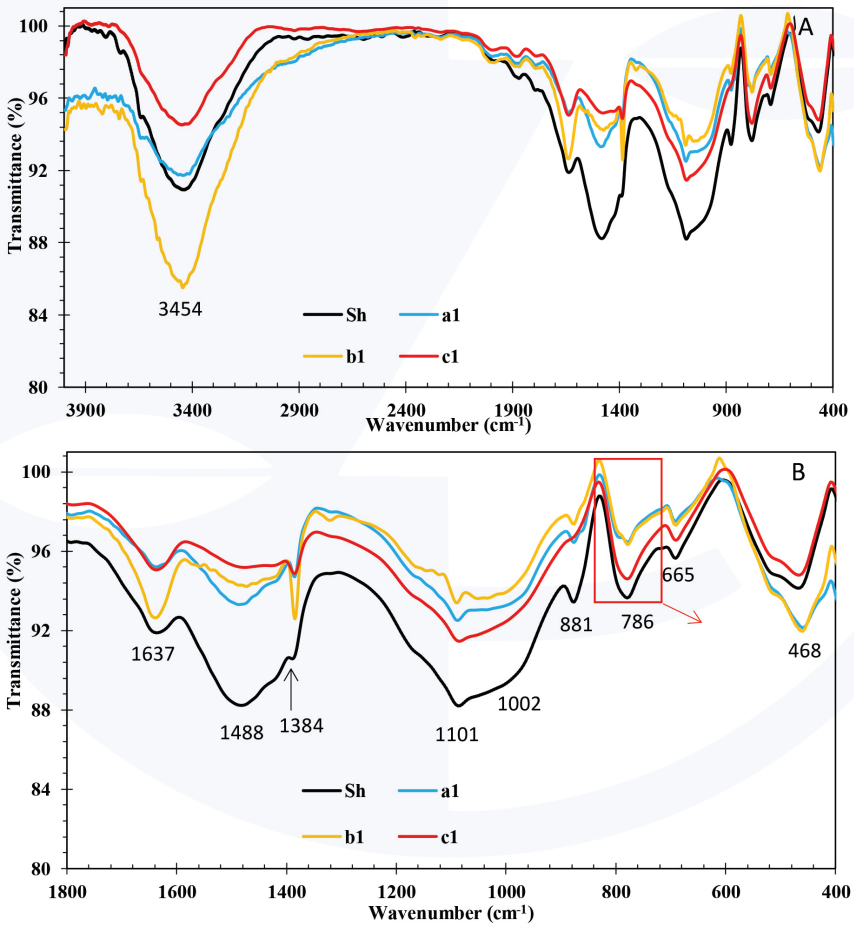

Figure 7- FTIR test results related to 28-day cement mortar sample. (A) the whole spectrum and (B) the range of 400 cm^{-1} to 1800 cm^{-1} (Sh is the Control)

In the spectra shown in Figure 7, in the studied samples, the peaks at wavelengths of about 3450 cm-1 and 1637cm-1 are related to the tensile and flexural vibrations of O-H bonds in adsorbed water molecules, respectively [10, 11]. Also, in these samples, the tensile vibra-

tions of the bonds in the carbonate group have shown the structure of calcium carbonate in the cement at a wave number of 1488 cm-1 absorption peak [12]. In addition, at the wavenumber 1384cm-1 the absorption peak related to the tensile vibrations of Si-O bonds in the anion units of SiO_4^{4-} can be seen [13]. The peaks at the wave numbers 1101 cm-1and 1002 cm-1 are related to the tensile vibration of Si-O-Si and Si-O-Al bonds in cement compounds, respectively [14]. In addition, at wave number 881 cm^{-1} the absorption peak is relat-ed to the tensile vibrations of the existing C-O bonds of calcite [15]. Comparing the peaks of calcium carbonate and silica peaks, it is clear that the control sample has more calcite and silica than the other samples.

The two peaks positioned at the wave numbers 665 cm^{-1} and 468 cm^{-1} are related to the flexural vibration of Si-O bonds in different compounds [13-16]. Also, as mentioned, the peak positioned at the wave number of 786 cm^{-1} is observed in the samples containing high amounts of alkali [13]. By comparing the peak intensity in this wave number, it is clear that samples a1 and b1 had the lowest, and control samples had the highest amount of alkali in the structure.

Another parameter introduced by Berra et al. is the Coefficient of Structural Disorder [17]. This coefficient is proposed to evaluate the sensitivity to alkaline reaction in cement before use and hydration. According to this coefficient, if the value of this parameter is less than 120, it means that the sample is inactive, if, between 120 and 200, it means the sample has little activity, if, between 200 and 300, it means it is highly active, and if more than 300, it means the sample has pozzolanic activity [17]. Since the used cement is type II and although it is inactive, the study of this factor during the reaction, which can indirectly represent CaOH2 or other alkaline compounds, can be useful. According to this theory, the value of this coefficient is obtained from Equation (1). [17]

$$C_d^{\,l} = \Delta v / A'_b \qquad (1)$$

In this equation, Cd is the coefficient of structural disorder and Δv is the peak width positioned at the wave number 796 cm-1and the value of A'b is extracted from Equation (2).

$$A'_b = \log [(P+Z)/Z] \qquad (2)$$

In this equation, P is the minimum peak point positioned at 796 cm^{-1} and Z is the difference between the minimum peak positioned at wave numbers 796 cm^{-1} and 1100 cm^{-1}. The value obtained for this coefficient is shown in the form of bar graphs in Figure 8 for better comparison.

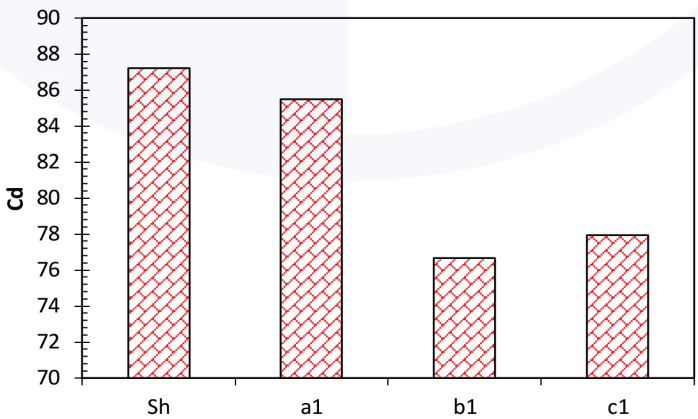

Figure 8- Values obtained for the Coefficient of the Structural Disorder for different samples at the age of 28 days. (Sh is the control)

According to the results obtained for this co-efficient, it is clear that the value of Cd for the control samples is the highest and for b1 samples is the lowest. Therefore, the obtained results in this study showed that the studied samples were in-active and that was consistent with the structure of the used cement. And the least chemical activ-ity belonged to sample b1 and the most chemical activity belonged to the control sample. This coefficient is used for the degree of alkalinity of different cements and here, despite the use of the same type of cement, a different amount of chemical composition is created.

The results of FT-IR test of samples 42 and 90 are shown in Figures 9 and 10. For better comparison, the results of the magnified image of these spectra in the range of 400 cm^{-1} to 1800 cm^{-1} are also shown.

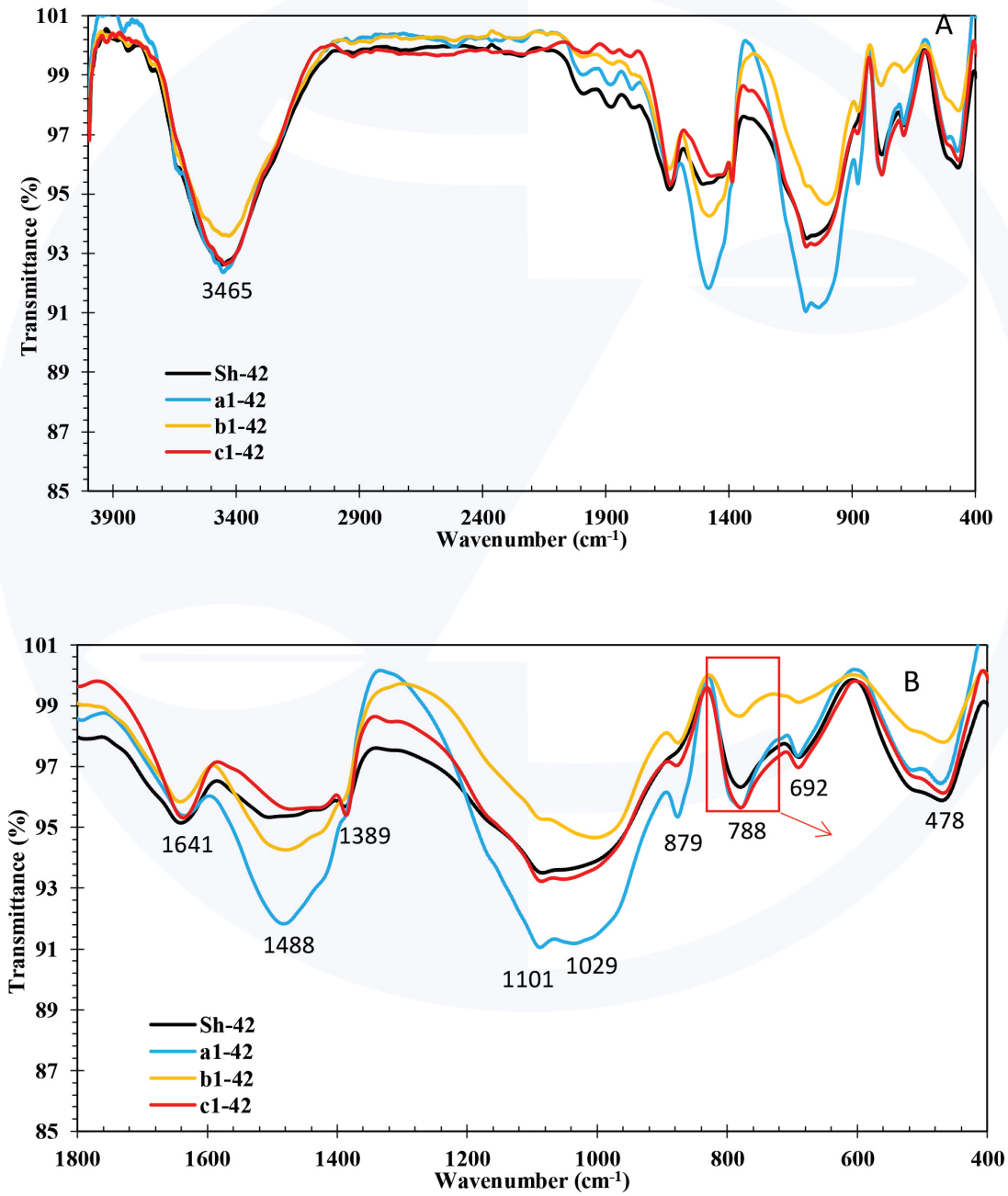

Figure 9- FTIR test results for sample 42 (A) of the whole spectrum and (B) the range of 400 cm^{-1} to 1800cm^{-1}. (Sh is the control)

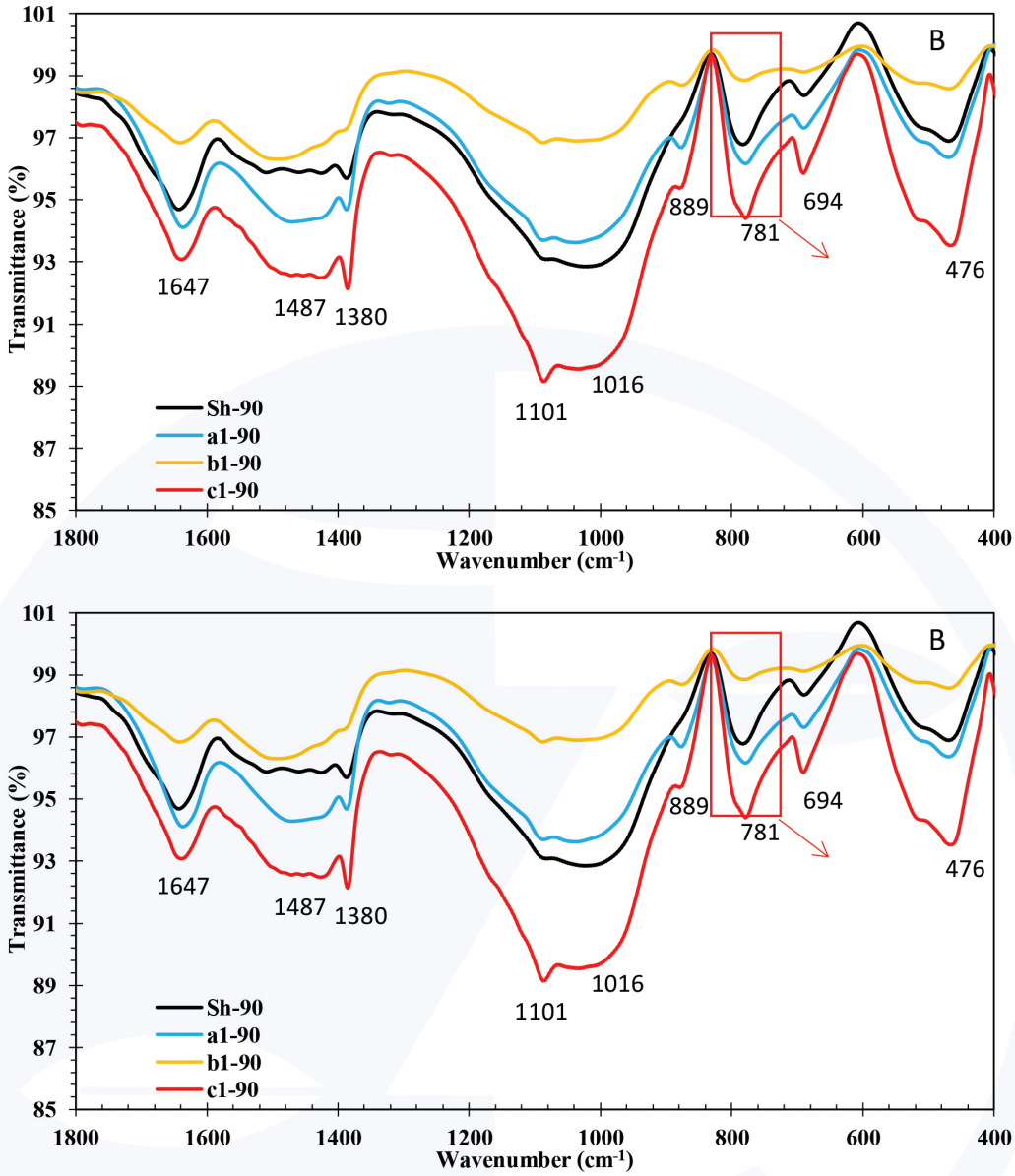

Figure 10- FTIR test results for sample 90 (A) of the whole spectrum and (B) the range of 400cm^{-1} to 1800cm^{-1} (Sh is the control)

In these two samples, the peaks at wave numbers of about 3450 cm^{-1} and 1640 cm^{-1} are again related to the tensile and flexural vi-brations of O-H bonds in adsorbed water molecules, respectively [10,11]. Also in these samples, the tensile vibrations of the bonds in the carbonate group have shown the structure of calcium carbonate in the cement at a wave number of 1488 cm^{-1} [12]. In the 42 day samples, the amounts of calcium carbonate in sample a1 are higher than in other samples.

This is while, in the 90-day samples, the amount of this substance was more in sample c1 than in sample a1. In addition, in the wave number of 1380 cm^{-1} to 1389 cm^{-1}, the absorption peak related to the tensile vibrations of Si-O bonds in the units of SiO44- anions can be seen in both samples [13]. However, in sample 90, this peak is intensified, which could indicate more abundance of sulfate anion in this sample. The peaks at the wave numbers about 1100 cm-1and 1020 cm^{-1} are related to the tensile vibration of Si-O-Si and

Si-O-Al bonds in the compounds in cement, respectively [14]. Here again, it is observed that the siliceous structures in samples a1 and c1 were the higher after 42 and 90 days, respec-tively. In addition, at a wave number of about 885 cm^{-1}, the absorption peak is related to the tensile vibrations of the existing C-O bonds of calcite [15].

The two peaks at wave numbers about 690 cm^{-1} and 470 cm^{-1} are also related to the flexural vibration of Si-O bonds in different compounds [13,16]. Also, as mentioned before, the peak positioned at the wave number about 781 cm^{-1} is observed in samples containing high amounts of alkali [13]. By comparing the peak intensity in this wave number, it is clear that sample b1 in both groups of 42 days and 90 days had the least amount of alkali in the structure. However, in the 42-day sample, the alkalinity of samples c1 and a1 was the same and more than the control value. Also, after 90 days, the amount of alkali in sample c1 was significantly more than in other samples. The value obtained for the Coefficient of the Structural Disorder of 42-day and 90-day samples is shown in the form of bar graphs in Figure 11,12 for better comparison [17].

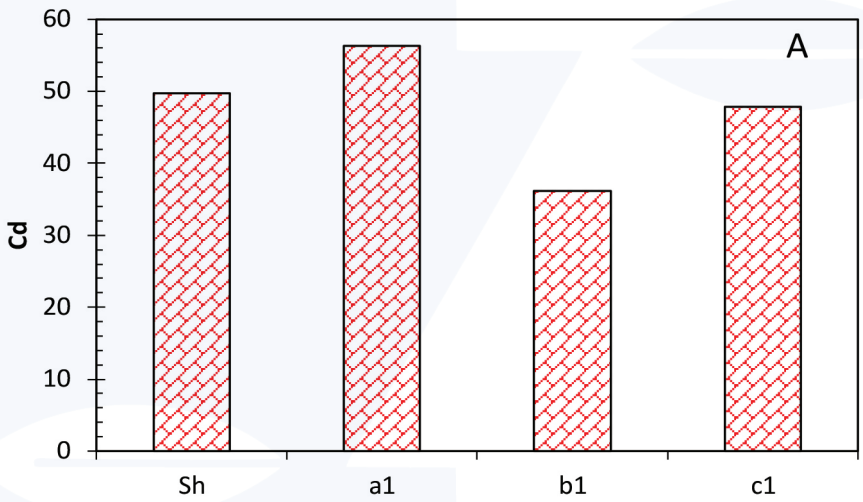

Figure 11- Values obtained for the Structural Disorder Coefficient of different samples at the age of 42 days (sh is the control)

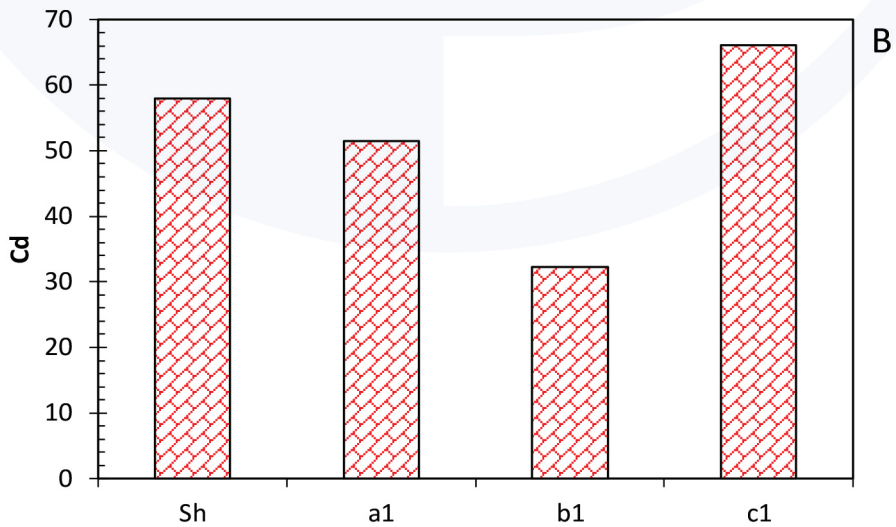

Figure 12- Values obtained for the Structural Disorder Coefficient of the samples at the age of 90 days (sh is the control)

According to the results obtained for this coefficient, it is clear that the value of Cd for samples a1 and c1 was higher after 42 and 90 days, respectively. Also, in both sample categories, the lowest value of this this coefficient belonged to sample b1. As previously stated, the value of Cd can be considered a measure of the alkaline-silica activity of a sample. And the least chemical activity, as mentioned before, be-longed to sample b1. These differences occurred while the used cement was the same in all samples. It should be noted that this coefficient can represent any type of alkali in these samples and the type of chemical composition cannot be explained.

XRD test of samples at the age of 90 days- Series 3

XRD test was used to investigate the crystal structure of the studied samples. The diffraction patterns are shown in Figure 13. The analysis information is as follows:

Reference Standard of the test:

BS EN 13925-1: 2008, Anode: Cu, Voltage: 40 KV, Current: 30 mA

Counting time:

0.5 sec, Step Size: 0.02, 2ɵ: 2-100°

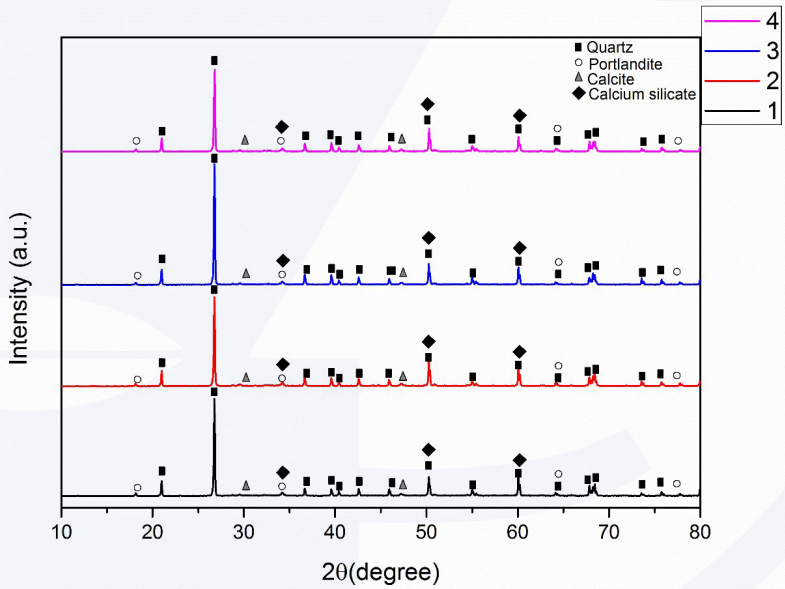

Figure 13- The diffraction patterns obtained from the four samples under study. (Control:4, l:cl, 2: al, 3: bl)

According to Figure 13, in all four samples, there were two predominant phases and two small phases. The predominant phases included one quartz phase (SiO_2) with referen ce code JCPDS No: 05-0490 and one portlandite phase (Ca (OH) 2) with reference code JCPDS No: 44-1481. Also, the other two phases present in the samples with a much lower value were calcite ($CaCO_3$) with reference code JCPDS No: 05-0586 and calcium silicate (Ca_3SiO_5) with reference code JCPDS No: 42-0551. The Rietveld method was used to measure the values of each phase in the samples. In this technique, by the least-squares method, the theoretical diffraction patterns are adapted to the values obtained from the test and thus the values of each phase are calculated. The results of this adaptation are reported in Table 3.

Table 3 . Percentage of chemical compounds in 90-day cement (4-sh is the control)

Sample name	SiO_2 (%)	Change to control %	$Ca(OH)_2$ (%)	Change to control %	$CaCO_3$ (%)	Change to control %	Ca_3SiO_5 (%)	Change to control %
1-c1	66.2	5%-	32.2	10.6%	0.9	80%	0.7	75%
2-a1	67.2	3.7%-	31.5	8%	0.8	60%	0.5	25%
3-b1	69.4	*	29.5	1%	0.6	20%	0.5	25%
4-sh	69.8	*	29.1	*	0.5	*	0.4	*

According to Table 3, it is clear that from samples 1 to 4, the value of SiO2 in the cement increased and the percentage of Ca $(OH)_2$ de-creased. Also, the other two phases from sam-ples 1 to 4 either decreased or did not change. Sample No. 4 is the control sample. In general, calcium-containing compounds have higher values under TCF.

During the hydration of cement after 90 days, it is expected that the chemical compounds con-taining CH and C-S-H to grow, as shown in Figure (14). Compared to the control sample, it seems that the formation of chemical com-pounds occurred more intensely, or, in other words, more complete hydration was formed under TCF.

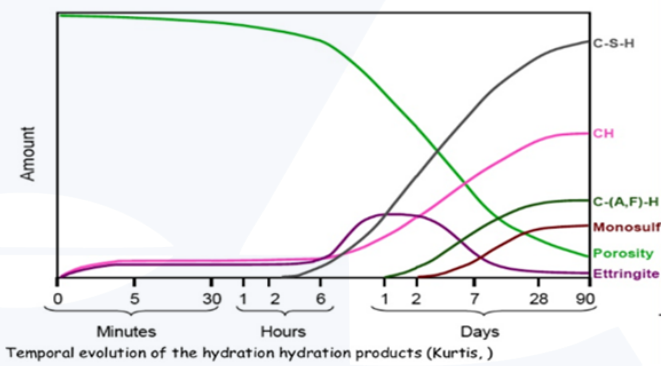

Figure 14- The process of creating chemical compounds in cement [18]

XRF and L.O.I analysis of 90-day sample -Series 3

XRF analysis was performed to evaluate the abundance of elements in the samples. Also, to examine the L.O.I (Loss on Ignition) of weight loss due to combustion, the samples were exposed to 950° C for 1.5 hours. The results of Percentage changes are presented in Table 4· Reference standard: ASTM E1621-13

Table 4 . Percentage of the elements in cement samples and amount of weight loss due to combustion

	Samples			
%Oxide/Name	c1	a1	b1	Sh-Control
Na_2O	0.04	0.06	0.08	0.11
Mg_2O	0.54	0.46	0.48	0.54
Al_2O_3	1.6	1.5	1.49	1.43
Si_2O_3	66.1	67	68.6	68.4
P_2O_5	0.07	0.14	0.14	0.18
SO_3	0.87	0.88	0.96	0.93
K_2O_3	0.11	0.14	0.09	0.16
Ca O	20.6	19.6	18.1	18.2
Fe2O3	3.1	2.9	2.9	3
L.O.I	6.97	7.32	7.16	7.05

Table 5 . Comparison of the percentage of the most elemental changes compared to the control

Oxide%	Samples			
	c1	a1	b1	Sh-Control
Na_2O	-64%	-45.45%	-27.27%	*
Al_2O_3	12%	5%	4%	*
$P2O_5$	-61%	-22%	-22%	*
K_2O_3	-45.50%	-12.50%	-43.80%	*
CaO	13.20%	7.70%	0	*

Table 5 shows the comparison of the percentage of some element changes in comparison to the control samples. One of the important points in Table 5 is the significant reduction of Potassium, Sodium, and Phosphorus in the samples under CF. Sodium (Na) and Potassium oxides (K) play an active role in the alkaline reaction of con-crete with aggregates and cause cracking and destruction of concrete [19]. The abundance of alkalis in cement is limited and mainly below 4%, however, this small amount has certain ef-fects on hardening behavior. With the increase of alkalis including Sodium and Potassium, the initial strengths increase, and the 28-day strengths decrease.

The reason is the effect of Potassium on the hydration of C3S [20]. The higher the C3S content in Portland cement, the faster this type of cement hardens. While, if the C2S is higher, the cement hardens at a lower rate. But in the end, it reaches a higher strength [20-21]. According to Table 5, in the samples under CF, the amount of Sodium (Na) and Potassium (K) has been reduced by approximately (~ 30%), and instead more CaO has been reported. Cement with more CaO starts to harden at a slower rate but reaches higher final strengths [20-21]. If this process has taken place from the be-ginning of hydration, it can be considered ef-fective in justifying the slow process of starting strength at 7 days and continuing to increase strength at older ages.

SEM analysis of the 90-day samples-Series 3

Finally, the SEM images are shown in figures 15-19. The images were taken from the samples in order to observe the crystal differences.

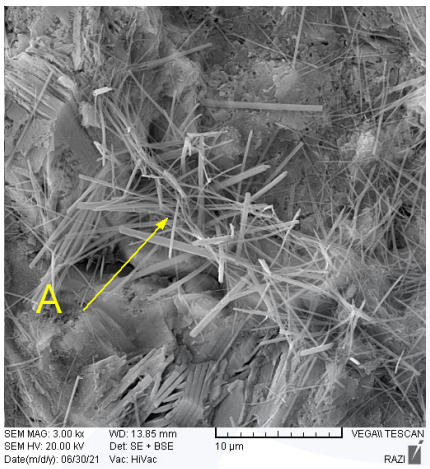

Spectra: sample A-A.spx

Element	Series	unn. C [wt.-%]	norm. C [wt.-%]	Atom. C [at.-%]
Oxygen	K series	34.05	37.40	57.07
Magnesium	K series	0.77	0.85	0.85
Aluminium	K series	4.57	5.02	4.54
Silicon	K series	10.66	11.71	10.18
Sulfur	K series	3.44	3.78	2.88
Calcium	K series	34.11	37.46	22.82
Iron	K series	3.45	3.79	1.66
Total:		91.0 %		

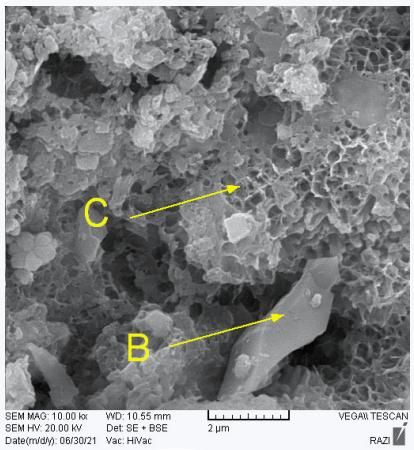

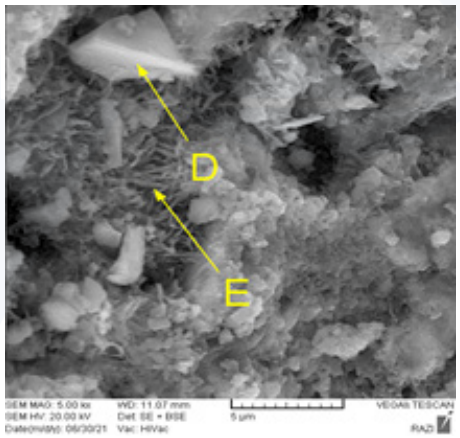

Spectra: sample A-B.spx

Element	Series	unn. C [wt.-%]	norm. C [wt.-%]	Atom. C [at.-%]
Oxygen	K series	37.61	45.46	67.19
Silicon	K series	16.48	19.92	16.77
Sulfur	K series	2.06	2.49	1.84
Calcium	K series	2.91	3.52	2.08
Iron	K series	23.68	28.61	12.12
Total:		82.7 %		

Spectra: sample A-D.spx

Element	Series	unn. C [wt.-%]	norm. C [wt.-%]	Atom. C [at.-%]
Oxygen	K series	65.72	62.04	75.66
Silicon	K series	28.69	27.09	18.82
Sulfur	K series	1.97	1.86	1.13
Calcium	K series	9.54	9.01	4.38
Total:		105.9 %		

Spectra: sample A-C.spx

Element	Series	unn. C [wt.-%]	norm. C [wt.-%]	Atom. C [at.-%]
Oxygen	K series	26.08	30.90	58.77
Silicon	K series	3.10	3.68	3.98
Sulfur	K series	1.98	2.35	2.23
Calcium	K series	2.55	3.02	2.29
Iron	K series	50.69	60.06	32.72
Total:		84.4 %		

Spectra: sample A-E.spx

Element	Series	unn. C [wt.-%]	norm. C [wt.-%]	Atom. C [at.-%]
Oxygen	K series	36.02	42.27	61.33
Magnesium	K series	3.00	3.52	3.36
Aluminium	K series	3.32	3.90	3.35
Silicon	K series	9.41	11.04	9.12
Sulfur	K series	1.58	1.85	1.34
Calcium	K series	30.94	36.31	21.03
Iron	K series	0.95	1.12	0.46
Total:		85.2 %		

Figure 15- Sample a1

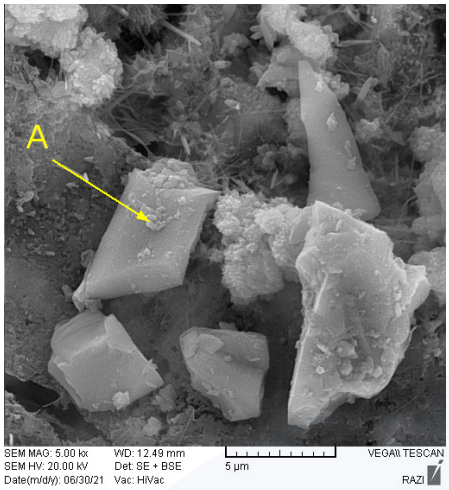

Spectra: sample B-A.spx

Element	Series	unn. C [wt.-%]	norm. C [wt.-%]	Atom. C [at.-%]
Oxygen	K series	52.96	58.90	73.20
Aluminium	K series	0.55	0.61	0.45
Silicon	K series	26.91	29.93	21.19
Calcium	K series	8.96	9.97	4.95
Iron	K series	0.53	0.59	0.21
	Total:	89.9 %		

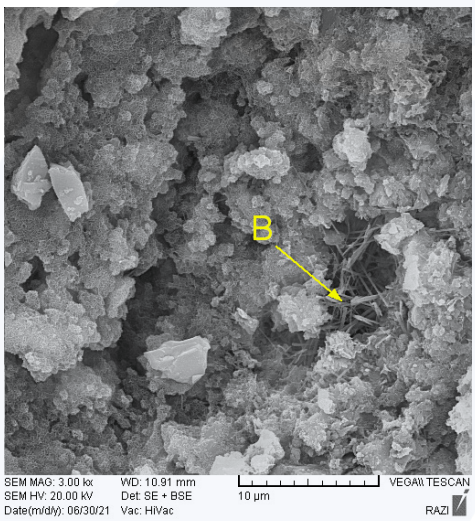

Spectra: sample B-B.spx

Element	Series	unn. C [wt.-%]	norm. C [wt.-%]	Atom. C [at.-%]
Oxygen	K series	32.20	41.31	61.74
Magnesium	K series	0.59	0.75	0.74
Aluminium	K series	1.79	2.30	2.04
Silicon	K series	4.29	5.50	4.68
Sulfur	K series	6.23	7.99	5.96
Calcium	K series	31.40	40.29	24.04
Iron	K series	1.45	1.85	0.79
	Total:	77.9 %		

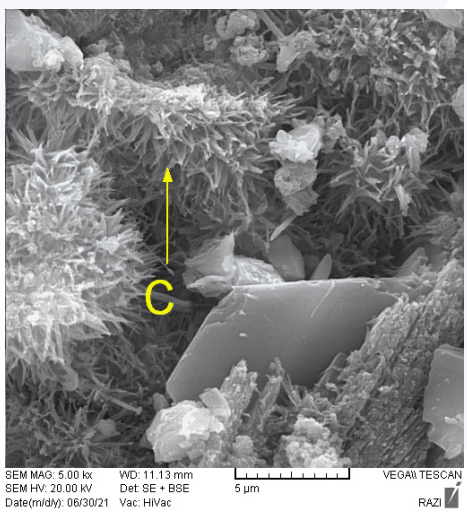

Spectra: sample B-C.spx

Element	Series	unn. C [wt.-%]	norm. C [wt.-%]	Atom. C [at.-%]
Oxygen	K series	46.45	51.06	70.31
Aluminium	K series	0.99	1.09	0.89
Silicon	K series	8.48	9.32	7.31
Sulfur	K series	3.51	3.86	2.65
Calcium	K series	30.24	33.24	18.27
Iron	K series	1.31	1.44	0.57
	Total:	91.0 %		

Figure 16- Sample bl

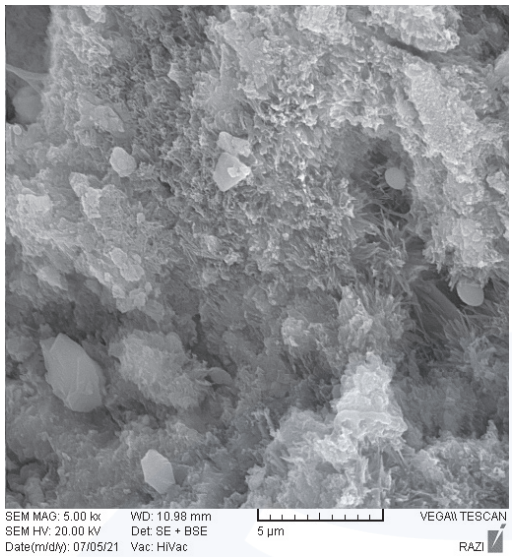

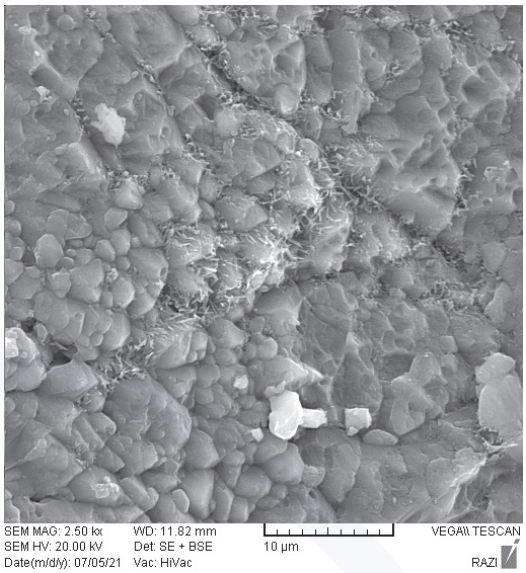

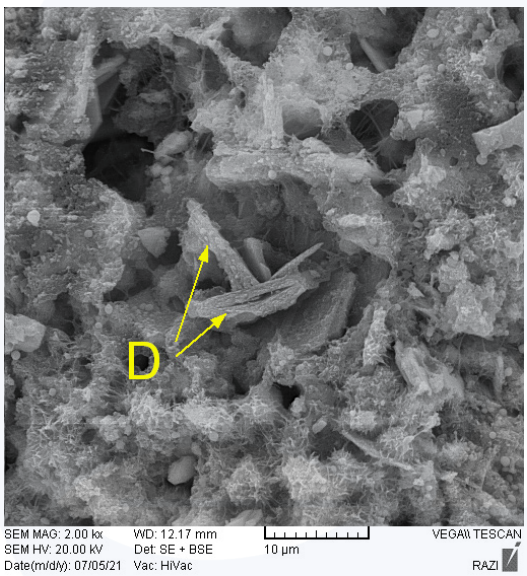

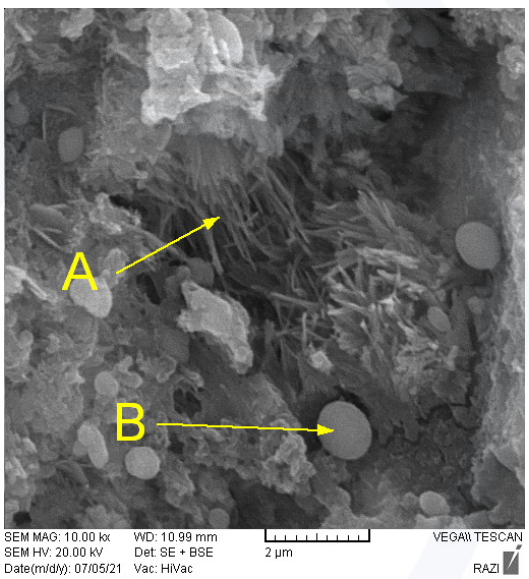

Spectra: sample C-D.spx

Element	Series	unn. C [wt.-%]	norm. C [wt.-%]	Atom. C [at.-%]
Oxygen	K series	47.79	50.79	69.95
Aluminium	K series	9.88	10.50	8.58
Silicon	K series	1.21	1.28	1.01
Calcium	K series	34.51	36.68	20.17
Iron	K series	0.71	0.75	0.30
	Total:	94.1 %		

Spectra: sample C-A.spx

Element	Series	unn. C [wt.-%]	norm. C [wt.-%]	Atom. C [at.-%]
Oxygen	K series	7.76	9.16	17.58
Magnesium	K series	2.39	2.82	3.56
Aluminium	K series	4.35	5.14	5.85
Silicon	K series	24.84	29.33	32.06
Sulfur	K series	3.99	4.71	4.51
Calcium	K series	37.52	44.29	33.93
Titanium	K series	0.20	0.23	0.15
Iron	K series	3.65	4.31	2.37
	Total:	84.7 %		

Spectra: sample C-B.spx

Element	Series	unn. C [wt.-%]	norm. C [wt.-%]	Atom. C [at.-%]
Oxygen	K series	9.53	14.08	28.10
Aluminium	K series	0.55	0.81	0.96
Silicon	K series	7.55	11.16	12.68
Sulfur	K series	2.32	3.43	3.42
Calcium	K series	43.43	64.18	51.13
Titanium	K series	0.57	0.84	0.56
Iron	K series	3.72	5.50	3.14
	Total:	67.7 %		

Figure 17- Sample c1

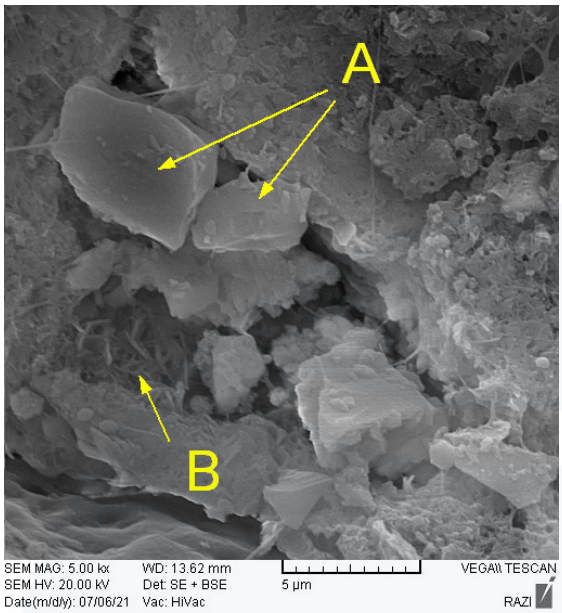

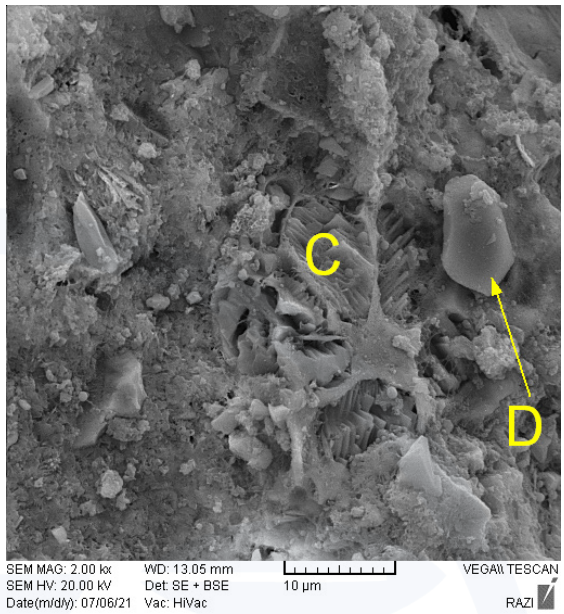

Spectra: sample SH-A.spx

Element	Series	unn. C [wt.-%]	norm. C [wt.-%]	Atom. C [at.-%]
Oxygen	K series	45.61	48.47	62.56
Sodium	K series	5.07	5.38	4.84
Magnesium	K series	0.20	0.22	0.18
Aluminium	K series	9.24	9.82	7.52
Silicon	K series	27.21	28.91	21.26
Potassium	K series	0.20	0.21	0.11
Calcium	K series	6.09	6.48	3.34
Iron	K series	0.48	0.51	0.19
Total:		94.1 %		

Spectra: sample SH-C.spx

Element	Series	unn. C [wt.-%]	norm. C [wt.-%]	Atom. C [at.-%]
Oxygen	K series	36.86	38.10	57.38
Magnesium	K series	1.95	2.02	2.00
Aluminium	K series	0.85	0.88	0.79
Silicon	K series	15.30	15.82	13.57
Sulfur	K series	2.72	2.81	2.11
Calcium	K series	38.38	39.67	23.85
Iron	K series	0.68	0.70	0.30
Total:		96.7 %		

Spectra: sample SH-B.spx

Element	Series	unn. C [wt.-%]	norm. C [wt.-%]	Atom. C [at.-%]
Oxygen	K series	27.30	32.89	51.07
Magnesium	K series	3.70	4.46	4.56
Aluminium	K series	2.56	3.09	2.84
Silicon	K series	14.52	17.49	15.47
Sulfur	K series	1.39	1.67	1.30
Calcium	K series	32.23	38.83	24.07
Iron	K series	1.30	1.56	0.70
Total:		83.0 %		

Spectra: sample SH-D.spx

Element	Series	unn. C [wt.-%]	norm. C [wt.-%]	Atom. C [at.-%]
Oxygen	K series	55.31	54.76	68.68
Aluminium	K series	0.36	0.36	0.26
Silicon	K series	39.11	38.72	27.67
Sulfur	K series	2.48	2.45	1.54
Calcium	K series	3.74	3.71	1.86
Total:		101.0 %		

Figure 18- Sample control Sh

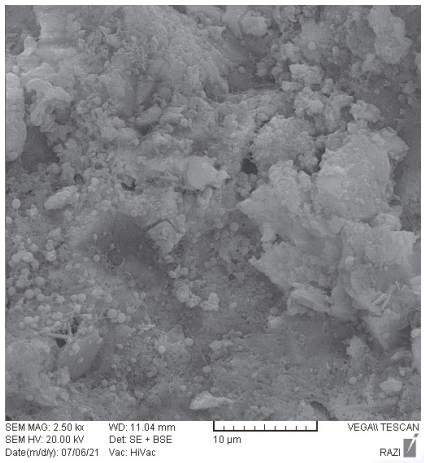

Spectra: sample SH-E.spx

Element	Series	unn. C [wt.-%]	norm. C [wt.-%]	Atom. C [at.-%]
Oxygen	K series	56.09	62.60	76.46
Silicon	K series	22.81	25.45	17.71
Calcium	K series	10.70	11.95	5.83
Total:		89.6 %		

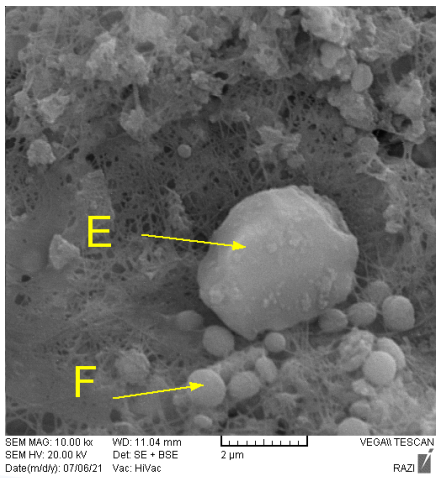

Spectra: sample SH-F

Element	Series	unn. C [wt.-%]	norm. C [wt.-%]	Atom. C [at.-%]
Oxygen	K series	48.52	49.14	68.04
Magnesium	K series	0.91	0.92	0.84
Aluminium	K series	1.77	1.80	1.47
Silicon	K series	12.99	13.16	10.38
Sulfur	K series	3.34	3.38	2.34
Calcium	K series	27.75	28.10	15.53
Iron	K series	3.46	3.50	1.39
Total:		98.7 %		

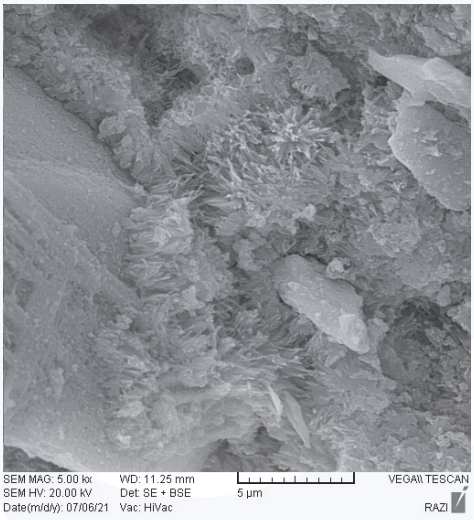

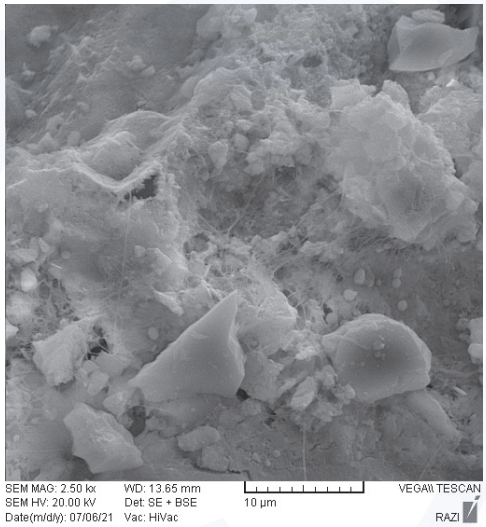

Figure 19- Sample control Sh

In the SEM images, the process of formation of crystals containing calcium, iron, aluminum, and sulfur is more clearly seen in the samples under the TCF and can indicate the formation of ettringite (Figures 15 to 19). The importance of this difference is illustrated in Figure (20) of the 90-day cement sample with 5 and 20% of fly ash, which shows the difference in ettringite formation. Wind ash is added to cement to reduce CO_2 and preserve the environment [22]. Ettringite is also a product of the combination of calcium aluminate with calcium sulfate, and its small amounts increase the strength, and high amounts will have a negative effect on the durability of concrete. Of course, the dimensions of the effect of Ettringite on the efficiency of cement are of interest to the industry and there is still a lot of work to be done in this regard. Some studies have been done to use the heat capacity of this compound in cement to optimize building heating [23-24].

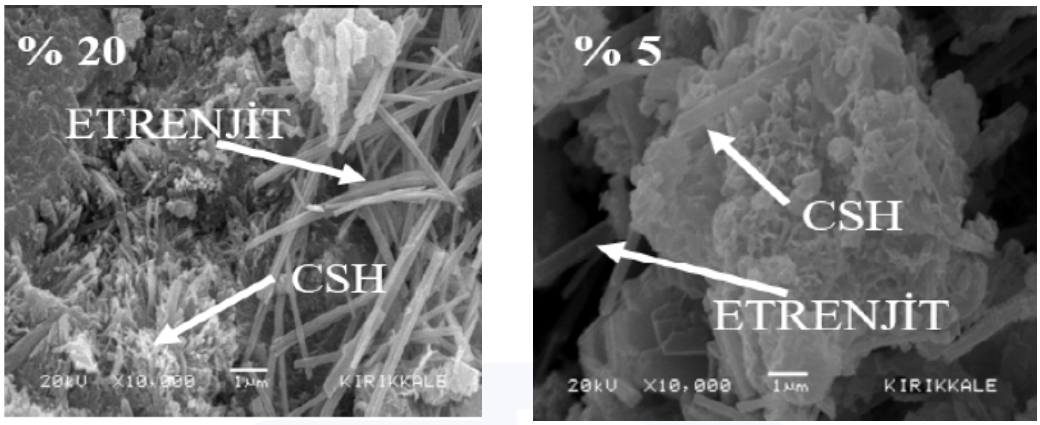

Figure 20- How crystals are formed in modified cement (green) with 5 and 20% fly ash at the age of 90 days [22]

Conclusion

As seen, in most of the samples under the TCF, the growth rate of strength over time compared to the age of 7 days was higher than in the control samples. This phenomenon shows changes in the structure of chemical compounds [25-26]. Examining the supplementary analyzes of Series 3, the followings are seen:

In XRD results, the abundance of silicon-containing compounds in the control sample is higher at 90 days. While, in the samples under the TCF, the predominant chemical compounds are mainly calcium. In the samples under CF, $CaCO_3$ compounds are 20 to 80% and Ca_3SiO_5 compounds are 25 to 75%, and also Ca (OH)2 is more formed.

From the XRF results, it is clear that the abundance of calcium and aluminum in the samples under TCF was higher (about 7% on average). Sodium (Na), Potassium (K), and Phosphorus (P) are about 30% on average (between 13 and 64%) less in the samples under TCF, which have special effects on delaying the hydration process (increasing long-term strength).

In SEM images, the process of ettringite mation is more clearly seen in the samples under TCF. Due to the fact that the composition of cement elements under the CF has changed (Table 5-6), the creation of new chemical compounds has a new trend and is not comparable to the conventional chemistry of cement.

A noteworthy point in the results of FT-IR analysis is that the change in chemical bonds for each sample is unique to that sample.

In general, the present study presents the following general points:

- From the SEM images and XRD results and comparison with the expected hydration process, it can be said that in total, at 90 days, we see more complete hydration in the samples under Consciousness Bond Field.
- XRF result show the change of the amount of elements in the samples under TCF. Considering that all samples are made of one material, change of elements is possible through the transformation of T-Consciousness into matter. One of the challenges of the concrete industry is to achieve the chemical compositon, the processing of materials close to the cement structure, which can be combined with known cements and have a favorable effect on the properties of cement. Consciousness Bond Field can create appropriate structural changes by making changes in the cement base using T-Consciousness and not material.
- In this research, the process of internal changes for each series and group is independent of others. However, the general change is in the direction of increasing strength, and this is in accordance with the theory of the General Connection of Particles,

which states that changes in the behavior of materials under the Consciousness Bond Field in order to improve their fundamental character [4]. And since the basic character of

- So far, in the experience of working with TCFs, we have found that the dimensions of achievement in their implementation are much more than a specific function. It means that when cement is placed under the TCF, other parameters and chemical compounds change in a multifaceted and completely targeted way [27-28].

This directly means changing behavior in different situations. In this respect, we are faced with a multifaceted technology that creates the possibility of different functions at the lowest cost, and this has always been the focus of the industry.

Acknowledgments

The authors would like to thank Dr. Bakhshi for his cooperation over the years.

References

1. Locher F.W. (2006) .Cement: principles of production and use ISBN9789642917020,pp13
2. U.S. (2012).Geological Survey, Mineral Commodity Summaries, January
3. Taheri.M.A . (2012).*General Connection of particles* .Interuniversal Publishing.Erfan-Halgheh. ID: 978-1-940491-03-5
4. Taheri.M., Payervand, F., Ahmadkhanlou, F., Torabi, S., & Semsarha, F. (2021). Distinction of Consciousness Fields According to Taheri from Other Conventional Physical Fields: Evaluating the Magnetic Properties of Materials.
5. Taheri M.A, (2013) .*Human from another outlook.* Interuniversal Press; 2nd Edition ISBN-13: 978-1939507006, ISBN- 10: 1939507006
6. WWW.Cosmointel.com
7. http://www.isiri.gov.ir, Iran Institute of Standards and Industrial Research
8. Joseph.Sh,Joseph.A.Mand Bishnoi.Sh,(2015). EconomicImplicationsofLimestoneClinkerCalcinedClayCement(LC3)inIndia,CalcinedClaysfor SustainableConcrete,RILEMBookseries10,DOI10.1007/978-94-017-9939-3_62
9. Scrivener K, FREng. Cement chemistry and sustainable materials(2018).Edx
10. Javidparvar A.A, Ramezanzadeh.B, Ghasemi.E,(2016). The effect of surface morphology and treatment of Fe3O4 nanoparticles on the corrosion resistance of epoxy coating, J. Taiwan Inst. Chem. Eng. 61 . https://doi.org/10.1016/j.jtice.2016.01.001.
11. Anchieta.C, Cancelier.A, Mazutti.M, Jahn. S, Kuhn.R, Gündel. A, O. Chiavone-Filho. O, Foletto.E,.(2014). Effects of Solvent Diols on the Synthesis of Zn-Fe2O4 Particles and Their Use as Heterogeneous Photo-Fenton Catalysts, Materials (Basel). 7 -6281–6290. https://doi.org/10.3390/ma7096281.
12. Sasnauskas. V,.(2013). Cement hydration with zeolite-based additive, Chemija. 24 - 271–278
13. Hassan.M,Khatib.J.M,Mangat.P.S,Naseef.A,Gardiner.P.H.E,.(2014).FTIRandXRDCharacterizedPortlandCementStabilisedLeadContaminatedSoil, in: Int. Conf. Nat.Sci.Environ.(ICNSE2014),Dubai,(:pp.102–106.)
14. Springfield.T;(2021). Application of FTIR for Quantification of Alkali in Cement, (2011) https://www.researchgate.net/publication/313389380_FTIR_and_ XRD_Characterized_Portland_Cement_Stabilised_Lead_Contaminated_Soil
15. Chollet.M,Horgnies.M;(2011). AnalysesofthesurfacesofconcretebyRamanandFT-IRspectroscopies:Comparativestudyofhardenedsamplesafter demoulding andafterorganicpost-treatment,Surf.InterfaceAnal.43-714–725.https://doi.org/10.1002/sia.3548.
16. Trezza M.A;(2007). Hydration study of ordinary Portland cement in the presence of zinc ions, in: Mater. Res. Universidade Federal de Sao Carlos, (pp. 331–334).https://doi.org/10.1590/S1516-14392007000400002.
17. Berra M, MangialardiT, Paolini A.E;.(1999). Rapid evaluation of the threshold alkali level for alkali-reactive sliceaous aggregates in concrete", Cement and Concrete Composites 21 -325-333
18. Scrivener K, FREng. Cement chemistry and sustainable materials, Edx-Introuction &Hydration(2018)
19. Zandi Y . (2009). Advanceed ConcreteTechnology (2009). ISBN:978-964-547-221-2. PP5-25
20. Locher F.W, (2006). Cement: principles of production and use ISBN:9789642917020-pp206
21. Taylor H.F.W, .(1997). Cement Chemistry, 2nd Ed. Academic Press, London
22. Demir. I, Guzelkuck.S, Sevim.O, Filaze.A, Sengul.C.G.(2017),Mortar Examination of Microstracture of Fly Ash in Cement Proceedings ofThe IRES International Conference, Lisbon, Portugal, 11th-12th December
23. Ndiaye K, Ginestet. S, Cyr.M;(2017). Durability and stability of an ettringite-based material for thermal energy storage at low temperature. Cem Concr Res(99:106–15) https://doi.org/10.1016/j.cemconres.2017.
24. Khadim.P, Gineste.N.S, Cyr.M, (2018). Experimental evaluation of two low temperature energy storage prototypes based on innovative cementitious material https://doi.org/10.1016/j.apenergy.2018.02.136
25. Locher. F.W, (2006) .*Cement: principles of production and use* -ISBN9789642917020,pp204
26. Double.D.D,(1983). New developments in understanding the chemistry of cement hydration, Published: Royal Societyhttps://doi.org/10.1098/
27. Kazazi.B,Taheri.M.A , (2001) Effects of the Consciousness Field on Concrete (ASR).
28. Kazazi.B, Taheri.M.A,(2021). Influence of the Consciousness Bond Field on alkaline reaction of Concrete